Evolution of Water Proton Nuclear Magnetic Relaxation during Milk Coagulation and Syneresis: Structural Implications

Charles Tellier,*,† François Mariette,‡ Jean-pol Guillement,§ and Philippe Marchal‡

Laboratoire de RMN et Réactivité Chimique, CNRS URA 472, and Département de Mathématiques, CNRS URA 758, 2 rue de la Houssinière, 44072 Nantes Cedex 03, France, and CEMAGREF, Division Technologie, 17 rue de Cucillé, 35044 Rennes Cedex, France

NMR transverse relaxation times of water were obtained in skim milk after renneting and during the syneresis of the curd. New data analysis using the maximum entropy method was applied to relaxation curves to investigate the distribution of water between the whey and the curd during the shrinkage of the milk clot. It is shown that the T_2 relaxation behavior is best presented as a continuous spectrum of relaxation times. Quantitative estimation of the amount of water inside the curd and in the whey can then be obtained at any stage of syneresis in an undisturbed way. Furthermore, transverse relaxation data were interpreted in terms of the microscopic structure of the water compartment inside the curd, and information about the water pore geometry and size distribution is deduced by inversion of NMR transverse relaxation data.

1. INTRODUCTION

Gels formed from milk by renneting under quiescent conditions may subsequently show syneresis whereby the whey component of milk is expelled following curd formation (Pearce and MacKinley, 1989). When cheese is made from renneted milk, syneresis is an essential step that affects the moisture content and the quality of the final product. So it is useful to understand and quantitatively describe syneresis, i.e., measure shrinkage and the amount of whey expelled. Existing methods to measure syneresis can be classified in two groups: measurements involving the physical separation of curd from whey (Beeby, 1959; Tarodo de la Fuente, 1969; Marshall, 1982) and measurements made while curd is still in the whey (Zviedrans and Graham, 1981). The inherent problem with separation methods is that curds tend to collapse when handled, which induces rapid expulsion of whey. Other methods require an added tracer which does not interfere with the process of syneresis or will not absorb to or diffuse through the curd.

NMR is a particularly attractive technique for such a heterogeneous system as it is both nondestructive and noninvasive. Proton NMR relaxation times have been extensively used to investigate the state of water under a wide variety of materials (Hills et al., 1990; Kakalis et al., 1990; Lambelet et al., 1989). NMR relaxation measurements have also been shown to be a sensitive probe in the study of morphological changes associated with aggregation and gelation as well as large scale changes induced, for example, by dehydration, freezing, and thawing (Hills et al., 1989b; Belton et al., 1988).

The purpose of this study is to interpret the proton T_2 relaxation time variation upon gelation of milk by rennet and subsequent syneresis. We present the analysis of the multiexponential relaxation behavior of water proton in curd by the maximum entropy method (MEM), which is more appropriate for the study of the relaxation than the common technique of fitting a limited sum of discrete T_2 components. Interpretation in terms of the microscopic structure of the curd is proposed.

2. THEORY

Proton relaxation times have been extensively used to study the state of water in food, but interpretation is highly model dependent. In the analysis of ^{1}H NMR relaxation data, it is necessary to consider the effects of cross relaxation between water molecules and protein protons as well as proton chemical exchange between protein ionizable groups, carbohydrate protons, and water molecules (Fedotov et al., 1969; Hills et al., 1989a, 1991). However, in the case of proton transverse relaxation, the contribution of cross relaxation is small and can be neglected.

Previous studies on skim milk (Lelièvre and Creamer, 1978; Roefs et al., 1989) show that proton transverse relaxation is mainly monoexponential, suggesting a fast diffusive exchange of water between the different compartments. A rather general model will consider three exchanging fractions of protons: (1) protons of "free" water molecules; (2) protons of water molecules ("bound" water) directly interacting with proteins; (3) exchangeable protein protons such as side-chain protons from OH, NH_2, and SH or exchangeable hydroxyl protons from carbohydrates. According to this model, if there is a rapid diffusive exchange between the protons of free water and bound water and an intermediate exchange between the proton of the OH groups and the water protons, the observed transverse relaxation rate at low field where the chemical shift differences of exchangeable protons are small is given by

$$1/T_2 = P_f/T_{2f} + P_b/T_{2b} + P_e/(T_{2e} + k_e^{-1}) \qquad (1)$$

where T_{2i} is the relaxation time of the different proton states, with P_i their relative population. k_e^{-1} is the mean lifetime of exchangeable protons on proteins or carbohydrates. This relation, which is also expected at high field in the short pulse spacing limit, is valid with

$$k_b^{-1} \ll T_{2b} \qquad P_f \gg P_b, P_e$$

where k_b^{-1} is the lifetime of water in the bound state.

* Author to whom correspondence should be addressed.
† Laboratoire de RMN et Réactivité Chimique.
‡ CEMAGREF.
§ Département de Mathématiques.

0021-8561/93/1441-2259$04.00/0

A quantitative description of the effect of chemical exchange can be obtained from the dependence of the water transverse relaxation rate on pulse spacing in the Carr–Purcell–Meiboom–Gill sequence at high field (Hills et al.,1989a). The resulting dispersive curve is analyzed in terms of variables characterizing the chemical exchange between water and protein/carbohydrate protons. At high field the additional variable is the frequency difference between the water and exchangeable protons $\delta\omega$ (rad^{-1}) which is related to the spectrometer frequency ω_o (MHz) by $\omega_0 = 2\pi\omega_0\delta$, where δ is the chemical shift difference in ppm. At very long pulse spacing, the relaxation is given by the modified Swift–Connick expression (Swift and Connick, 1962):

$$\frac{1}{T_{2obw}} = \frac{P_f}{T_{2f}} + \frac{P_b}{T_{2b}} + P_e k_e \left[\frac{T_{2e}^{-2} + T_{2e}k_e + (\delta\omega)^2}{(T_{2e} + k_e)^2 + (\delta\omega)^2} \right] \quad (2)$$

In the limit of very short pulse spacing, chemical shift differences do not contribute to relaxation and the observed relaxation rate reduces to eq 1. Between the limit cases a modified expression (Carver and Richards, 1972) must be used.

In a protein gellike curd, water molecules are confined by the protein network in pores or cavities (Guthy et al., 1989). Then, relaxation time measurements can be sensitive to the morphology of the system and pore geometry and size can be determined (Davies and Packer, 1990; Davies et al., 1990; Whittall, 1991). The simplest physical model is the "two-fraction fast–exchange model" (Zimmerman and Brittin, 1957; D'Orazio et al., 1989) which assumes that there are two magnetically distinct phases within the pore: a bulk phase with relaxation characteristic of the bulk fluid and a surface phase where water molecules within a certain distance λ from the surface exhibit an enhanced relaxation. Possible mechanisms for the enhancement are slower tumbling of bound water near the surface, anisotropic motion of bound water (Farrell et al., 1989), or chemical exchange between water and proton from the matrix. Assuming that diffusion of water is faster than the relaxation processes, the observed relaxation rate for a given pore is

$$1/T_{2obs} = P_f/T_{2f} + P_s/T_{2s} \quad (3)$$

where f and s represent the bulk and surface water. When the majority of water is contained in the bulk phase (i.e., $P_f \gg P_s$), the equation may be rewritten in terms of the surface area, S, and the volume, V, of the water cavity.

$$1/T_{obs} = 1/T_{2f} + (S/V)(\lambda/T_{2s}) \quad (4)$$

If the diffusion between the water cavities in the gel is restricted during the time of the NMR experiment, the different pores can be considered as being independent. Assuming a surface relaxation rate constant over the entire sample, relaxation time measurements can provide the pore size distribution. The water in each individual pore has its own relaxation rate which depends linearly on the surface-to-volume ratio of the particular pore. For the ith pore

$$1/T_{2i} = 1/T_{2f} + (S/V)_i(\lambda/T_{2s}) \quad (5)$$

For the entire sample, each of these relaxation rates contributes to the magnetization decay $M(t)$ in the spin–echo experiment and we obtain

$$M(t) = \int P(d) \exp\left[-t\left(\frac{1}{T_{2f}} + \frac{\lambda}{T_{2s}} \frac{m}{d} \right) \right] dd \quad (6)$$

where $P(d)$ is the pore size distribution function; d is the pore size, and m is a constant which depends on the geometry of the pores, assuming that the volume and the surface of a pore are proportional to d^3 and d^2, respectively ($m = 4$ for a cylindrical geometry). The transverse relaxation time T_{2f} of the bulk water can be independently measured; if the ratio λ/T_{2s} is known, then $P(d)$ can be found by inversion of eq 6. For practical purposes, the inversion of the magnetization data is performed on a modified version of eq 6

$$A(t) = \int F(T) \exp(t/T) dT \quad (7)$$

where

$$A(t) = M(t) \exp(1/T_{2f})$$

$A(T)$ represents the time dependence of the reduced magnetization after the contribution from bulk relaxation has been subtracted and $T = T_{2s}d/\lambda m$.

The pore size distribution $P(d)$ is then obtained from the distribution of the relaxation time $F(T)$ using

$$P(d) = T_{2s}/\lambda m F(T) \quad (8)$$

This model to approach the pore size distribution is only valid in the fast diffusion regime where the time taken to diffuse to the surface is short compared with the surface relaxation strength, and then the relaxation behavior is uniform over the entire pore. This condition implies that

$$\lambda/T_{2b} \ll D/d \quad (9)$$

where D (m^2/s) is the self-diffusion coefficient of the bulk water.

3. MATERIALS AND METHODS

3.1. Materials. Reconstituted skim milk was prepared from a low heat skim milk powder (Nizo) at 9% (w/w); 0.02% of a rennet solution (1% in acetate buffer, pH 5.5, 0.02% NaN_3) was added and well mixed to 20 mL of milk sample. The milk was allowed to clot directly in the NMR tube (40-mm diameter). This large NMR tube prevented the gel from sticking to the wall of the tube and allows syneresis to occur within 10 h. When a standard NMR 10-mm tube is used, no syneresis is observed.

3.2. NMR Measurements. During syneresis, all measurements were performed on a Bruker PC110 operating at 10 MHz without spinning the sample. Transverse relaxation times (T_2) were measured using the standard Carr–Purcell–Meiboom–Gill pulse sequence, and the resulting magnetization decay curve was sampled with 800 points. To analyze the dependence of transverse relaxation rate on the 90–180 pulse spacing, experiments were carried out at a higher magnetic field on a modified WM 250 Bruker spectrometer allowing single point acquisition during the spin–echo experiments. The 90–180 pulse spacing was varied between 50 μs and 5 ms, the relaxation delay was 8 s, and relaxation curves were the mean of 4 accumulations at 10 MHz and 32 accumulations at 250 MHz.

Self-diffusion coefficients were measured by the pulse field gradient technique (Stejskal and Tanner, 1965) at 20 MHz on a minispec Bruker PC120 equipped with the field gradient unit. This technique involves the application of two identical rectangular field gradient pulses before and after the 180° refocusing pulse of the Hahn echo sequence ($90°_x$–τ–$180°_y$–τ-echo). An echo attenuation for unrestricted Brownian motion is observed in function of the time, Δ, between the field gradient pulses corresponding to the time of diffusion

$$I(G)/I(0) = \exp[\gamma^2\delta^2G^2D(\Delta - \delta/3)] \quad (10)$$

where γ is the gyromagnetic ratio for the hydrogen and δ (500 μs) and G (2.3 T/m) are, respectively, the duration and the magnitude of the magnetic field gradient pulse. The echo attenuation in curd was measured at 2τ = 160 ms.

3.3. Data Analysis. The general equation describing multiexponential transverse relaxation is

$$M(t_i) = \int F(T_2) \exp\left(\frac{t_i}{T_2}\right) dT + \epsilon_i \qquad i = 1, 2, ..., N \quad (11)$$

where the N data $M(t_i)$ are measured at times t_i, $F(T_2)$ is the unknown amplitude of the spectral component with relaxation T_2, and ϵ_i is the noise component with a zero mean value and a known standard deviation σ. The extraction of $F(T_2)$ from the observed magnetization, $M(t_i)$, requires the solution of eq 11, which is a Fredholm integral equation of first kind. For computer implementation, eq 11 is transformed in a finite sum of M exponential decays with relaxation times T_j and amplitude P_j

$$M(t_i) = \sum_{j=1}^{M} P_j e^{-t_i/T_j} + \epsilon_i \qquad i = 1, 2, ..., N \quad (12)$$

To determine P_j and T_j, we first used classical non-linear reconvolution and least-squares analysis such as the Marquardt algorithm or the Laplace–Pade methods (Marquardt, 1963; Tellier et al., 1991), where the magnetization decay is analyzed according to eq 12 with a minimal number of discrete exponential terms ($M < 5$) until the lowest possible χ^2 is reached.

Because the true relaxation spectrum $F(T_2)$ is more likely to be continuous, reflecting the continuous distribution of water cavities in curd, we also used the maximum entropy method (MEM) (Jaynes, 1982), which allows no restrictive prior assumptions about the number of exponential components in the data and introduces the least correlations in the reconstructed distribution from noisy data. Recently, the method was applied successfully to the ill-conditioned problem of inversion of Laplace transform in pulse fluorometry (Livesey et al., 1987) or the Fourier transformation of NMR spectra (Laue et al., 1985).

For computer implementation, we used the method of Skilling and Bryan (1984), where the entropy is defined as

$$S = -\sum_{j=1}^{M} P_j(\log P_j/A - 1)$$

where A is the initial guess of P_j, which is set to a flat distribution in T_2 space when one has no a priori knowledge about the distribution $F(T_2)$. The method searchs for a distribution which maximizes the entropy function under the constraint $\chi^2 = N\sigma^2$.

The function $Q(\lambda)$

$$Q(\lambda) = -S + \lambda\chi^2$$

is minimized for different values of the Lagrange multiplier λ which are gradually increased until the χ^2 is close to $N\sigma^2$.

4. RESULTS AND DISCUSSION

4.1. Effect of Milk Clotting on Water Transverse Relaxation Time. When rennet is added to the milk, the enzyme proceeds to cleave the κ-casein in the micelles and a hydrophilic macropeptide is released. In the case of skim milk, after most of the "hair" has been removed, steric and electrostatic repulsions between micelles are considerably reduced and flocculation proceeds leading to a gel (Walstra and Van Vliet, 1986). Microscopy (Green et al., 1978) reveals that the gel network originally consists of strands of micelles which evolve by fusion to ultimately form a giant paracasein "micelle" with holes containing water.

During this process, transverse relaxation remains monoexponential and no change in the relaxation time is detected (Table I) at either 10 or 250 MHz. This unexpected behavior had been already pointed out by Lelievre and Creamer (1978) and contrasts with the T_2 change observed during acid coagulation (Roefs et al., 1989). We recently demonstrated (Mariette et al., 1993) that water relaxation in milk can be interpreted by considering a fast exchange between free water, bound water, and exchangeable protons from protein and carbohydrates (see Theory). The lack of variation in T_2 could be explained by an exact compensation between the variation of P_b,P_e and T_{2b},T_{2e} (eq 1) during rennet coagulation of milk. To analyze the exact contribution of bound water and exchangeable protons to relaxation before and after the milk is renneted, we carried out relaxation measurements at higher field where a proton chemical exchange mechanism introduces a dependence of the proton transverse relaxation rate on pulse spacings in the CPMG pulse sequence (Figure 1). The gelation process does not significantly affect the dispersive curve for the milk, and the parameters for the exchange process determined by multiple parameter fitting remain very similar. These results demonstrated that the chemical exchange processes are not modified by milk gelation. Upon gelation, the relaxation time of protons in the protein matrix is usually reduced by hindering the rotational averaging of the proton dipolar interaction. Thereby, $1/T_{2e} \gg \delta\omega$ and the relaxation rate should be dominated by the fast relaxation of exchangeable protons or anisotropically bound water and given by eq 1. If exchangeable protons of the protein matrix contribute to the relaxation, we should observe a reduction in the amplitude of dispersive after milk coagulation. We can conclude that only exchangeable protons from soluble protein and carbohydrates (Hills, 1991; Lai and Schmidt, 1991) from whey are responsible for the dispersive shape of the curves. These molecules stay in the liquid serum inside the casein network so that the observed relaxation is not modified. As expected, the transverse relaxation dispersion of the rennet whey shows similar features to the milk one and we observed similar amplitude of the variation of relaxation

Table I. T_2 Relaxation Times of the Whey, Skim Milk, and Renneted Milk before and after Syneresis at 10 MHz (40 °C) and 250 MHz (20 °C)

	T_2 (ms)		
		250 MHz	
sample	10 MHz	short t_{cp}[a]	long t_{cp}
whey	1800 ± 20	422 ± 46	146 ± 4
skim milk, pH 6.6	200 ± 2	143 ± 5	79 ± 1
renneted skim mik before syneresis	200 ■ 2	148 ± 6	80 ± 1
renneted skim milk[b]	1800 ± 20	nd[c]	nd
after syneresis	67 ± 0.5		

[a] t_{cp} corresponds to the pulse spacing in the CPMG sequence. [b] Mean relaxation time values obtained from the bimodel relaxation spectrum obtained 400 min after renneting. [c] Not determined.

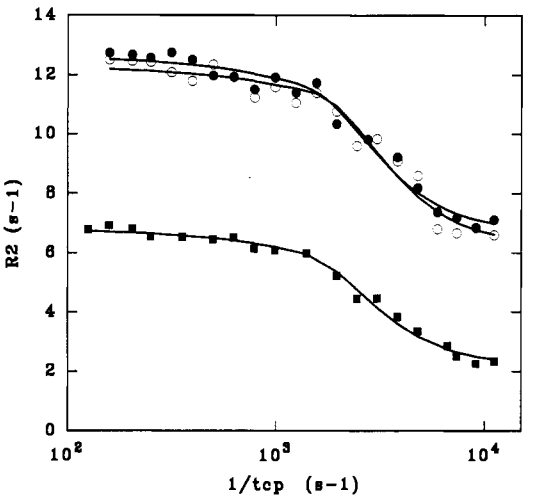

Figure 1. Experimental and calculated transverse proton relaxation dispersions for the skim milk at pH 6.6 (●), $P_e = 5.8 \times 10^{-3}$, $k_e = 1.8 \times 10^3$ s^{-1}, $\delta\omega = 2.25$ ppm, $T_{2a} = 0.226$ s, $T_{2b} = 2$ ms; the renneted skim milk at pH 6.6 (○), $P_e = 5.7 \times 10^{-3}$, $k_e = 1.8 \times 10^3$ s^{-1}, $\delta\omega = 2.62$ ppm, $T_{2a} = 0.243$ s, $T_{2b} = 2$ ms; and the rennet whey (■), $P_e = 4.6 \times 10^{-3}$, $k_e = 1.8 \times 10^3$ s^{-1}, $\delta\omega = 2.18$ ppm, $T_{2a} = 2$ s, $T_{2b} = 2$ ms. Experiments were carried out at constant temperature (20 °C) and spectrometer frequency (250 MHz).

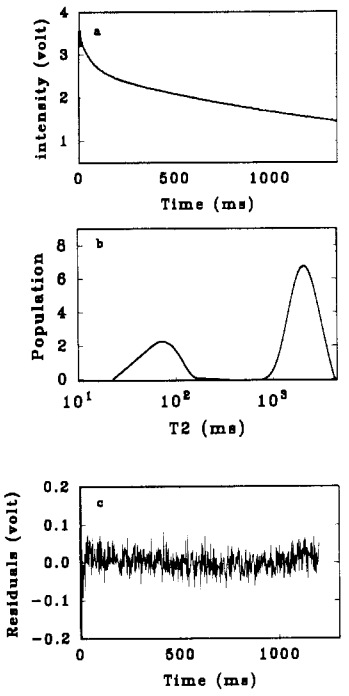

Figure 2. 10-MHz CPMG data (a) and the fit from a MEM reconstructed continuous T_2 spectrum (b) for the rennetted skim milk after syneresis (331 min) at 40 °C. (c) Plot of the residuals.

time upon pulse spacing ($1/T_{2\,\text{short pulse spacing}} - 1/T_{2\,\text{long pulse spacing}} \approx 4.5$–5) which only depends on the exchangeable variables (T_{2e}, T_e, k_e, and $\delta\omega$). The shift in relaxation rate between the curve from rennet whey and milk depends on the importance of the $P_f/T_{2f} + P_b/T_{2b}$ term, i.e., the amount of bound water. As we have already demonstrated (Mariette et al., 1993), milk micelles trapped a large amount of hydrated water with modified relaxation rate due to the presence of colloidal phosphocalcium complexes inside micelles. Whey proteins also trap water (Pessen et al., 1985) but to a lesser extent due to the low concentration of soluble protein (0.5%). Upon rennet gelation, no shifts in the dispersion curves are detected and the amount of bound water does not seemed to be affected (Figure 1). This result is consistent with previous observations demonstrating that the hydration of protein is unaffected by gelation (Tarodo de la Fuente et al., 1969) and that the colloidal phosphocalcium stays in the flocculated paracasein micelles (Walstra et al., 1985).

4.2. Evolution of Relaxation Rate during Syneresis. When milk clots by rennet action, the coagulum initially encloses the entire aqueous phase of the milk. After a few minutes at 40 °C in the NMR tube, the whey component of the milk starts to be expelled as the coagulum contracts. As soon as the whey is exuded from the gel, transverse relaxation curves can no longer be analyzed in terms of a single exponential component (Figure 2). Discrete deconvolution of the relaxation curve gives two T_2 components with relative amplitudes P_j, which depend on the time of syneresis (Figure 3). At the late stage of syneresis when most of the whey is expelled, better deconvolution, based on χ^2 misfit, is obtained with three discrete relaxation times. Analysis of the CPMG decay curve (Figure 2a) by the maximum entropy method (MEM) gives a bimodal spectrum (Figure 2b) with a continuous distribution of relaxation time at any time of the syneresis. The chi-square misfit (χ^2) is excellent, and close inspection of the residuals indicates that noise has not been incorporated in the fit (Figure 2c).

Figure 4 reports the evolution of the relaxation times

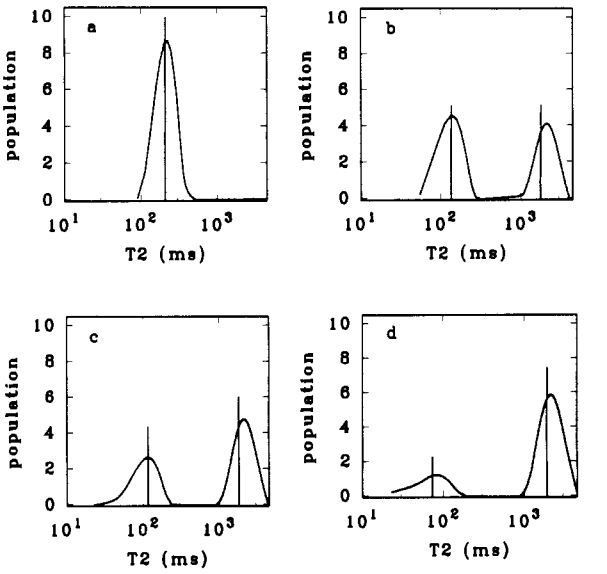

Figure 3. MEM reconstructed continuous T_2 and the corresponding discrete fit for the rennetted skim milk before syneresis (a) and during the time course of syneresis at 40 °C: (b) 137 min; (c) 200 min; (d) 405 min. Amplitude of the discrete fit was divided by a factor of 10.

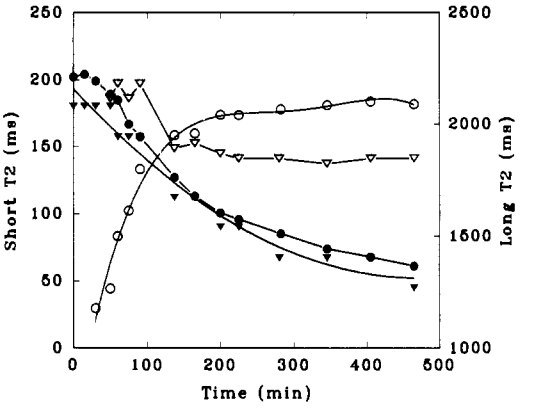

Figure 4. Evolution of the water transverse relaxation times as a function of time after renneting at 40 °C and 10 MHz. Solid symbols refer to the component with short relaxation time determined by MEM analysis (▼) and biexponential deconvolution (●). Open symbols refer to the component with long relaxation time determined by MEM analysis (▽) and biexponential deconvolution (○).

as a function of time of syneresis, obtained with the discrete and the continuous analysis. The agreement between the two methods is good for the evolution of the short relaxation time component. For the component with long relaxation time, discrete analysis shows a time-dependent evolution of the relaxation, whereas continuous deconvolution gives a nearly constant relaxation time which corresponds to the relaxation time of the rennet whey ($T_2 \approx 1800$ ms).

To understand this apparent discrepancy, we tested the two deconvolution methods with simulated CPMG relaxation data corresponding to two relaxation spectra: a discrete spectrum composed of two delta functions (simulation 1) and a continuous bimodal Gaussian spectrum (simulation 2) representative of spin–spin relaxation of water in milk during syneresis. Both spectra had the same total integral equal to 100 arbitrary units, and data corresponding to each spectrum were generated at $N = 600$ equally spaced times t_i with an added uncorrelated noise (standard deviation $\sigma_i = 0.02\%$). Table II summarizes the results obtained with various amplitude ratios of the two relaxation components. When the simulated

Table II. MEM and Discrete Analysis of Different Simulated CPMG Relaxation Curves Obtained from a Discrete Spectrum Composed of Two Delta Functions (T_{2a} = 90 ms and T_{2b} = 1000 ms) (Simulation 1) and from a Continuous Bimodal Gaussian Spectrum (Simulation 2)[a]

	simulated parameters amplitude (%)		calculated parameters: discrete analysis T_2 (ms)		discrete analysis amplitude (%)		MEM analysis T_2[b] (ms)		MEM analysis amplitude[c] (%)	
	a	b	a	b	a	b	a	b	a	b
simulation 1	90	10	90	1000	90	10	80	910	91	9
discrete spectrum	80	20	90	1000	80	20	80	890	82	18
T_{2a} = 90 ms	70	30	90	999	70	30	80	950	71	29
T_{2b} = 1000 ms	50	50	90	999	50	50	80	910	51	49
	40	60	90	999	40	60	84	832	40	60
simulation 2	90	10	83	424	83	17	80	910	90	10
continuous spectrum	80	20	82	595	75	25	80	890	81	19
T_{2a} = 90 ms	70	30	83	693	69	31	80	880	71	19
T_{2b} = 1000 ms	50	50	83	799	50	50	80	880	51	49
σ = 0.3[d]	40	60	84	832	40	60	80	880	41	59

[a] The relative amplitude of the two relaxation components was varied according to the observed relative variation during syneresis. CPMG curves were generated at N = 600 equally spaced times t_i with an added uncorrelated noise (σ = 0.02%). [b] T_2 values corresponding to the maxima in the relaxation spectrum. [c] Amplitude calculated from the integral of the broad T_2 relaxation dispersion. [d] σ is the relative standard deviation of the simulated Gaussian distribution.

data correspond to a discrete spectrum, the two methods (discrete analysis and MEM) recover the two components with roughly the right relaxation times and relative amplitudes. In the case of simulated data obtained with a continuous distribution, discrete analysis failed to recover the right value of the long relaxation time, especially when this component has a low relative amplitude; the lower the amplitude of the long component, the larger the bias on the relaxation value. From these simulated data, it is apparent that discrete analysis of relaxation curves does not correctly recover the maximum in case of a continuous spectrum of relaxation times. Moreover, a systematic error is introduced in one relaxation value which could be misinterpreted in term of physical sample modifications.

We can now interpret the time evolution of the long relaxation time during the syneresis (Figure 3) as a mathematical deconvolution artifact of the discrete analysis with no physical meaning. Furthermore, it seems that a continuous distribution of relaxation times is more appropriate to describe the rennet milk sample during syneresis, especially the relaxation of water inside the clot (see section 4.3).

The two peaks in the continuous spectra of Figure 3 can be related to the location of water in the sample. The peak corresponding to a long constant T_2 increases as syneresis occurs (Figure 4), and its relaxation time is close to the relaxation time of the rennet whey sampled at the end of syneresis. This peak is therefore associated with the whey expelled during syneresis. Concomitantly, the peak associated with the short relaxation time corresponds to the water trapped in the milk clot. In the time scale of the NMR measurements, no diffusive exchange between these two water compartments seems to occur since the long relaxation time is independent of the amount of whey expelled. As the proton NMR signal is directly proportional to the amount of resonant spins, the percentage of the two relaxation components is directly related to the amount of water inside and outside the gel.

From the above discussion, it follows that the quantitative interpretation of the proton relaxation spectrum could lead to a rapid and nondisturbing method to follow syneresis. The amplitude of each of the relaxation components is directly related to the amount of whey expelled or the shrinkage of the curd. Figure 5 gives an example of syneresis kinetics at 40 °C for skim milk followed by measurement of the relaxation amplitude of the water inside the clot. The interpretation of syneresis

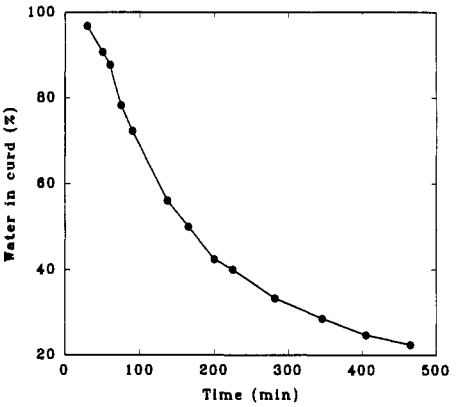

Figure 5. Water content of the curd determined by the relative amplitude of the short relaxation component as a function of the time after renneting. Temperature was kept constant at 40 °C.

kinetics strongly depends on the physical model used to describe the phenomenon and also on the method used to follow the syneresis (Walstra et al., 1985). However, our NMR method needs no handling of the gel during syneresis, and this process can be followed while the curd is still in the whey. The second advantage of the NMR method is that the time course of syneresis can be monitored from the very beginning of syneresis, when whey just starts to be expelled, until the complete shrinking of the curd. The last stage of syneresis is usually difficult to estimate by methods measuring the amount of water expelled or estimating the water (or dry matter) content of the curd because the whey never drains off completely, which implies that syneresis is underestimated.

4.3. Diffusion and Relaxation of Water inside the Curd. Before the milk is renneted, the transverse water proton relaxation is single exponential (Table I) because the microheterogeneity introduced by the casein micelles is too small to induce a slow diffusive exchange between the water inside the micelles and the lactoserum. The criterion for the observation of multiexponential relaxation in a heterogeneous system is dependent on the detailed geometry, but a good approximation of the limit is given by (Belton and Hills, 1987)

$$\Delta R_2 a^2/D > 1$$

a is the dimension of the heterogeneity (micelle radius = 0.05 μm), D the diffusion coefficient which is of the order of that of bulk water in milk (3×10^{-5} cm^2 s^{-1} at 40 °C),

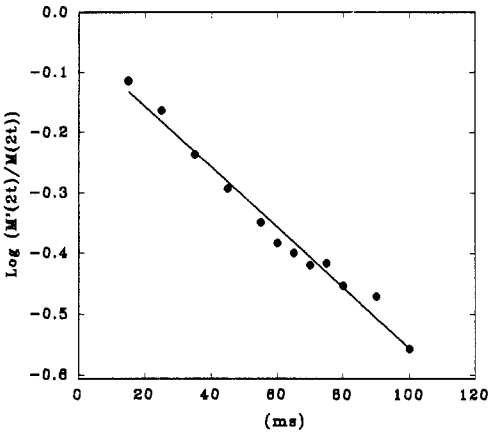

Figure 6. Spin–echo attenuation for the curd after syneresis as a function of the diffusion time Δ (ms) at 20 °C. G = 2.3 T/m, δ = 0.5 ms, echo time 2τ = 160 ms.

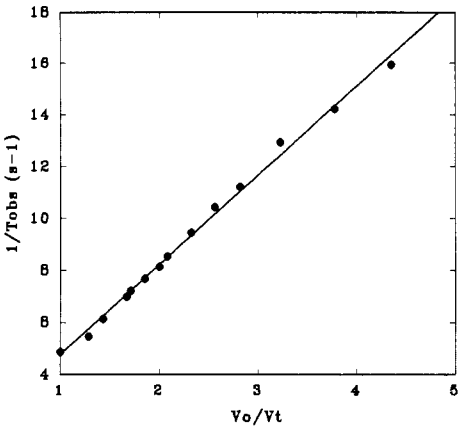

Figure 7. Dependence of the water transverse relaxation time inside the curd as a function of the inverse of relative water volume inside the curd during the time course of syneresis at 40 °C. The good linear fit (r^2 = 0.996) implies that fast exchange conditions (eq 4) apply to water relaxation in curd.

and ΔR_2 the difference between the water relaxation rate inside the micelles and in the lactoserum. We have demonstrated (Mariette et al., 1993) that the relaxation time of bound water in micelles is of the order of a few milliseconds so that fast diffusion regime is observed.

Upon gelation of milk by rennet, a single-exponential transverse relaxation is still observed (Table I), indicating that the fast diffusion regime is still fulfilled in the gel before syneresis. As proton relaxation mechanisms do not change with gelation (section 4.1), we can conclude that the microscopic heterogeneity of the gel is very small and still of the order of magnitude of micelle size. This result is justified by the investigations of the gel microstructure showing that in the early stage of gelation the gel matrix consists of strands of paracasein micelles (Walstra and Van Vliet, 1986).

As syneresis occurs, water relaxation time inside the gel becomes shorter and is characterized by a broad distribution in the continuous spectra of Figure 3. This distribution of relaxation times could either originate from a distribution of independent water cavities inside the gel in which water is in the fast diffusion regime or from an intermediate or a slow diffusion regime where the time for a water molecule to diffuse is long compared to the rate of surface relaxation ($\Delta R_2 a^2/D > 1$).

To detect possible restriction of water diffusion inside the gel, we measured the water self-diffusion coefficient with the pulse field gradient technique on the rennet whey and on the curd at 40 °C after syneresis. The echo attenuation data on curd (Figure 6) which were obtained over the range 20–100 ms show no curvature and give a self-diffusion coefficient D (2.15 × 10^{-5} cm^2 s^{-1}) which is slightly reduced compared to the water diffusion in rennet whey. Such behavior indicates that water molecules are free to move over distances up to $(6D\Delta)^{1/2} \approx 36$ μm and that there is no evidence of confinement of water into small pockets. This long-range motion of water inside the gel suggests that water moves in three dimensions by means of interconnected channels. Furthermore, reduction of the observed diffusion coefficient occurs both because of occasional binding at the protein matrix and because of a "tortuosity effect" which is determined by the local dimensionality. The one-third reduction factor of the diffusion factor in the curd is compatible with the cylindrical or capillary geometry (Callaghan et al., 1983).

The fast diffusion of water in curd indicates that water relaxation processes are in the fast diffusion regime in the curd unless the heterogeneity inside the gel is superior to a few micrometers. Equation 4, which is valid in the fast-exchange conditions, supposes that the observed relaxation rate should be related to the surface to volume ratio of the water compartment inside the curd, assuming that the bulk and surface relaxation times remain unchanged during syneresis. Figure 7 shows a linear relationship between the observed relaxation rate ($1/T_{obs}$) and the inverse of the relative amount of water inside the curd determined by multiexponential deconvolution of the signal at different times of syneresis. The protein surface (S) is supposed to be constant as the protein concentration of the whey does not change during the syneresis (Weber, 1984). This result clearly demonstrates that water relaxation inside the gel can be analyzed with the simple two-state model in fast exchange.

4.4. Compartment Sizes within the Curd. According to eq 6, the Laplace inverse transform of the magnetization decay should give the pore size distribution within curd assuming that T_{2f}, λ/T_{2s}, and m are known. T_{2f}, which is the relaxation time of bulk water also corresponds to the relaxation time of the rennet whey (≈1.8 s). m is related to the geometry of the structure and was set to 4 according to the cylindrical dimensionality of the water compartment suggested by the diffusion studies (section 4.3). The surface relaxation strength, λ/T_{2s}, is more difficult to evaluate. This value can be estimated from eq 4 applied to the clot milk before syneresis starts

$$1/T_2 = 1/T_{2f} + (S_0/V_0)(\lambda/T_{2s})$$

where S_0 is the total hydration surface of the protein network and V_0 the total volume of water inside the gel. The contact area between water and proteins in cheese has been estimated to be ≈700 m^2/g (Callaghan et al., 1983). Our milk samples have a casein concentration of 31 g/L so that the ratio S_0/V_0 is calculated to be 2.1 × 10^7 m^{-1}. The surface relaxation strength is then evaluated to ≈ 2 × 10^{-7} ms^{-1}. At this point, we emphasize that we assume that the surface relaxation stength is homogeneous throughout the curd sample, at least for distances longer than the diffusion length. This hypothesis is supported by the fact that transverse relaxation is still monoexponential after milk clotting by rennin, demonstrating a very short scale of microheterogeneity within the sample. In previous studies (Mariette et al., 1993) we have estimated the transverse relaxation time (1–3 ms) for the bound water. If this value is used for T_{2s}, we can derive the thickness of the water layer affected by the protein surface ($\lambda \approx$ 2–6 Å), which roughly corresponds to one or two layers of water molecules. This result is in good agreement

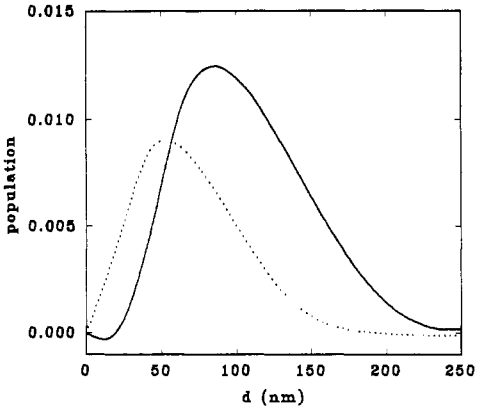

Figure 8. Water channel size distribution in curd after syneresis, 200 min (—) and 405 min (- - -), determined by MEM inversion of eq 6.

with previous calculations on different samples such as cheese (Callaghan et al., 1983) or porous silica glasses (D'Orazio et al., 1989).

Figure 8 represents the capillary size distribution $P(d)$ obtained from the relaxation data by Laplace inversion of eq 6 with a numerical algorithm using the maximum entropy principle. The size distributions are obtained at various times of syneresis and indicate that the mean capillary diameter reduces from 100 to 50 nm with the clot shrinkage. The accuracy of the method depends on a reliable estimation of the surface relaxation strength (λ/T_{2s}). However, this work and a previous one (D'Orazio et al., 1989) indicate that there is good evidence that this value does not vary greatly over a wide range of samples.

4.5. Conclusions. NMR relaxation analysis using numerical inversion methods under maximum entropy control has been shown to be a very powerful method for determining microstructural information in curd in a noninvasive way. This last advantage is of particular importance in studying gel structure such as curd which is very sensitive to mechanical manipulation and unstable during the time. We have demonstrated that water in clotted skim milk diffuses rapidly through the protein network in cavities with cylindrical or capillary geometry of mean diameter within 50–100 nm. The method is rapid as transverse relaxation curve measurement and signal analysis require less than 5 min with a standard personal microcomputer. Other structural techniques such as microscopy require a large quantity of two-dimensional information to extract the desired three-dimensional structure information.

The method could be of great use in rapid structural characterization of various food gels. Particularly, microstructural differences between milk clot obtained by acid or rennet coagulation are under investigation with this method.

ACKNOWLEDGMENT

This work was supported in part by Grant 89G0595 from the Ministère de la Recherche et de la Technologie and the Conseil Regional de Bretagne. We thank C. Braud for technical assistance.

LITERATURE CITED

Beeby, R. A method for following the syneresis of measuring the syneresis of rennet curd. *Aust. J. Dairy Technol.* **1959**, *14*, 77–79.

Belton, P. S.; Hills, B. P. The effects of diffusive exchange in heterogeneous systems on NMR lines shapes and relaxation processes. *Mol. Phys.* **1987**, *61*, 999–1018.

Belton, P. S.; Hills, B. P.; Raimbaud, E. R. The effects of morphology and exchange on proton NMR relaxation in agarose gels. *Mol. Phys.* **1988**, *63*, 825–842.

Callaghan, P. T.; Jolley, K. W.; Humphrey, R. S. Diffusion of fat and water in cheese as studied by pulsed field gradient nuclear magnetic resonance. *J. Colloid Interface Sci.* **1983**, *93*, 521–529.

Carver, J. P.; Richards, R. E. A general two-site solution for the chemical exchange produced dependence of T_2 upon the Carr Purcell pulse separation. *J. Magn. Reson.* **1972**, *6*, 89–105.

Davies, S.; Packer, K. J. Pore size distributions from nuclear magnetic resonance spin-lattice relaxation measurements of fluid-saturated porous solids. I. Theory and simulation. *J. Appl. Phys.* **1990**, *67*, 3163–3170.

Davies, S.; Kalam, M. Z.; Packer, K. J.; Zelaya F. O. Pore-size distributions from nuclear magnetic resonance spin-lattice relaxation measurements of fluid-saturated porous solids. II. Applications to reservoir core samples. *J. Appl. Phys.* **1990**, *67*, 3171–3176.

D'Orazio, F.; Tarczon, J. C.; Halperin, W. P.; Eguchi, K.; Misusaki, T. Application of nuclear magnetic resonance pore structure analysis to porous silica glass. *J. Appl. Phys.* **1989**, *65*, 742–751.

Farrell, H. M., Jr; Pessen, H; Kumosinski, T. F. Water interaction with bovine caseins by hydrogen-2 nuclear magnetic resonance relaxation studies: structural implications. *J. Dairy Sci.* **1989**, *72*, 562–574.

Fedotov, V. D.; Miftakhutdinova, F. G.; Murtazin, S. H. F. Investigation of proton relaxation in live plant tissues by the spin echo method. *Biofizika* **1969**, *14*, 873-882.

Green, M. L.; Hobbs, D. G.; Morant, S. V; Hill, V. A. Intermicellar relationships in rennet-treated separated milk. II. Process of gel assembly. *J. Dairy Res.* **1978**, *45*, 413–422.

Guthy, K.; Auerswald, D.; Buchheim, W. Electron microscopic and viscosimetric studies of the primary phase of rennet coagulation of milk. *Milchwissenschaft* **1989**, *44*, 560–563.

Hills, B. P. Multinuclear NMR studies of water in solutions of simple carbohydrates. I. Proton and deuterium relaxation. *Mol. Phys.* **1991**, *72*, 1099–1121.

Hills, B. P.; Takacs, S. F.; Belton, P. S. The effects of proteins on the proton NMR transverse relaxation times of water. I. Native bovine serum albumin. *Mol. Phys.* **1989a**, *67*, 903–918.

Hills, B. P.; Takacs, S. F.; Belton, P. S. The effects of proteins on the proton NMR transverse relaxation times of water. II. Protein aggregation. *Mol. Phys.* **1989b**, *67*, 919–937.

Hills, B. P.; Takacs, S. F.; Belton, P. S. A new interpretation of proton NMR relaxation time measurements of water in food. *Food Chem.* **1990**, *37*, 95–111.

Hills, B. P.; Cano, C.; Belton, P. S. Proton NMR relaxation studies of aqueous polysaccharide systems. *Macromolecules* **1991**, *24*, 2944–2991.

Jaynes, E. T. On the rationale of maximum-entropy methods. *Proc. IEEE* **1982**, *70*, 939–952.

Kakalis, L. T.; Baianu I. C.; Kumosinski, T. F. Oxygen-17 and proton nuclear magnetic relaxation measurements of soy protein hydration and protein-protein interactions in solution. *J. Agric. Food Chem.* **1990**, *38*, 639–646.

Lai, H.-M.; Schmidt, S. J. Proton, deuterium, and oxygen-17 nuclear magnetic resonance relaxation studies of lactose- and sucrose-water systems. *J. Agric. Food Chem.* **1991**, *39*, 1921–1926.

Lambelet, P.; Berrocal, R.; Ducret, F. Low resolution NMR spectroscopy: a tool to study protein denaturation. 1) Application to diamagnetic whey proteins. *J. Dairy Res.* **1989**, *56*, 211- 222.

Laue, E. D.; Skilling, J.; Staunton, J.; Sibisi, S.; Brereton, R. G. Maximum entropy method in nuclear magnetic resonance spectroscopy. *J. Magn. Reson.* **1985**, *62*, 437–452.

Lelievre, J.; Creamer, L. K. A pulsed NMR study of the formation and syneresis of renneted milk gels. *Milchwissenschaft* **1978**, *33*, 73–76.

Livesey, A. K.; Delaye, M.; Licinio, P.; Brochon, J. C. Maximum entropy analysis of dynamic paramaters via the Laplace transform. *Faraday Discuss. Chem. Soc.* **1987**, *83*, 247–258.

Mariette, F.; Tellier, C.; Brulé, G.; Marchal, P. Multinuclear NMR study of the pH dependent water state in skim milk and caseinate solutions. *J. Dairy Res.* **1993**, *60*, 175–188.

Marquardt, D. W. An algorithm for least squares estimations of nonlinear parameters. *J. Soc. Ind. Appl. Math.* **1963**, *11*, 431–441.

Marshall, R. J. An improved method for measurement of syneresis of curd formed by rennet action on milk. *J. Dairy Res.* **1982**, *49*, 329–336.

Pearse, M. J.; MacKinlay, A. G. Biochemical aspects of syneresis. A review. *J. Dairy Sci.* **1989**, *72*, 1401–1407.

Pessen, H.; Purcell, J. M.; Farrell, H. M., Jr. Proton relaxation rates of water in dilute solutions of β-lactoglobulin. Determination of cross-relaxation and correlation with structural changes by the use of two genetic variant of a self-association globular protein. *Biochim. Biophys. Acta* **1985**, *828*, 1–12.

Roefs, S. P. F.M.; Van As, H.; Van Vliet, T. Pulse NMR of casein dispersion. *J. Food Sci.* **1989**, *54*, 704–708.

Skilling, J.; Bryan, R. K. Maximum entropy image reconstruction: general algorithm. *Mon. Not. R. Astron. Soc.* **1984**, *211*, 111–124.

Stejskal, E. O.; Tanner, J. E. Spin diffusing measurements: spin echoes in the presence of a time dependent field gradient. *J. Chem. Phys.* **1965**, *42*, 288–292.

Swift, T. J.; Connick, R. E. NMR relaxation mechanisms of ^{17}O in aqueous solutions of paramagnetic cations and the lifetime of water molecules in the first coordination sphere. *J. Chem. Phys.* **1962**, *37*, 307–320.

Tarodo de la Fuente, D.; Alais, C.; Frentz, R. Study of the coagulating of milk by rennet and curd syneresis by the thromboelastographic method. *Lait* **1969**, *487*, 400–416.

Tellier, C.; Guillou-Charpin, M.; Le Botlan, D.; Pelissolo, F. Analysis of low resolution, low-field NMR relaxation data with the Pade-Laplace method. *Magn. Reson. Chem.* **1991**, *29*, 164–167.

Walstra, P.; Van Vliet, T. The physical chemistry of curd making. *Neth. Milk Dairy J.* **1986**, *40*, 241–259.

Walstra, P.; Van Dijk, H. J. M.; Geurts, T. J. The syneresis of curd. 1. General considerations and litterature review. *Neth. Milk Dairy J.* **1985**, *39*, 2O9–246.

Weber, F. In *Le fromage*; Eck, A., Ed.; Lavoisier: Paris, 1984; Chapter 2.

Whittall, K. P. Recovering compartment sizes from NMR relaxation data. *J. Magn. Reson.* **1991**, *94*, 486–492.

Zimmerman, J. R.; Brittin, W. E. Nuclear Magnetic resonance studies in multiple phase systems: Lifetime of a water molecule in an absorbing phase on silica gel. *J. Phys. Chem.* **1957**, *61*, 1328–1333.

Zviedrans, P.; Graham, E. R. B. An improved tracer method for measuring the syneresis of rennet curd. *Aust. J. Dairy Technol.* **1981**, *36*, 117–120.

Received for review March 26, 1993. Accepted September 23, 1993.[⊗]

[⊗] Abstract published in *Advance ACS Abstracts*, November 1, 1993.